01 Dec 1984

# The Oxidation Of Dilute Alloys Of Magnesium In Aluminium

Hollis P. Leighly
*Missouri University of Science and Technology*

A. Alam



## Recommended Citation

H. P. Leighly and A. Alam, "The Oxidation Of Dilute Alloys Of Magnesium In Aluminium," *Journal of Physics F: Metal Physics*, vol. 14, no. 6, pp. 1573 - 1583, article no. 024, IOP Publishing, Dec 1984.
The definitive version is available at https://doi.org/10.1088/0305-4608/14/6/024

# The oxidation of dilute alloys of magnesium in aluminium

J. Phys. F: Met. Phys. **14** (1984) 1573–1583. Printed in Great Britain

# The oxidation of dilute alloys of magnesium in aluminium

H P Leighly Jr† and A Alam‡

† Department of Metallurgical Engineering, University of Missouri–Rolla, Rolla, Missouri 65401, USA

‡ School of Mathematics and Physics, University of East Anglia, Norwich NR4 7TJ, UK

Received 19 July 1983, in final form 28 November 1983

**Abstract.** The oxide layers developed during the oxidation of aluminium alloys containing 500 and 1000 PPM of magnesium at 850 K were examined with the aid of electron spectroscopy for chemical analysis. The magnesium content of the oxide layers was relatively high because of the preferential depletion of the magnesium atoms from the base alloys. Near the outer surfaces of the oxide layers, spinel ($MgAl_2O_4$) was the predominant magnesium-bearing compound. At depth, MgO was more dominant.

The preferential depletion of magnesium from the alloys injected vacancies into the material. This led to the formation of defect clusters. The presence of these defect clusters explains the experimental observations reported earlier by other researchers.

## 1. Introduction

In a paper published recently by Alam *et al* (1982), the annealing of a severely quenched aluminium–500 PPM magnesium alloy was studied with the aid of Doppler broadening positron annihilation spectroscopy (West 1979). It was found that the $S$ parameter (West 1979) as a function of temperature showed a strong dependence on the pre-annealing atmosphere. (For a fuller explanation of the $S$ parameter, see the appendix.) If a very dry, high-purity nitrogen atmosphere ($\leqslant 10$ PPM $O_2$) was used for annealing before the specimens were severely quenched, the $S$–$T$ curves exhibited a relatively small, low-temperature $S$-parameter shelf followed by a peak at about 225 K, after which there was a rapid decline in $S$. Specimens that were annealed in very dry nitrogen containing 500 PPM oxygen before they were severely quenched produced a curve that had a much higher $S$-parameter low-temperature shelf and a higher peak at a somewhat higher temperature that was followed by a much slower, gradual decline at still higher temperatures. The presence of oxygen in the annealing atmosphere retarded the annealing of quenched-in defects. Specimens annealed in very dry air gave essentially the same $S$–$T$ curves as those heated in very dry, impure nitrogen.

Alam *et al* (1982) and Alam and West (1982) also performed extensive studies of the annealing behaviour of quenched aluminium, aluminium–zinc and aluminium–silicon alloys which were pre-annealed in different controlled atmospheres before being quenched. They concluded from their studies that of the alloys investigated only aluminium–magnesium was affected by having an impurity in the pre-annealing atmosphere, and this impurity must be oxygen.

Mechanical polishing to remove about 0.01 cm from the surfaces of the aluminium–magnesium specimens originally annealed in the less pure nitrogen did not

0305-4608/84/061573 + 11$02.25  

remove the effect even after the specimens were given a second annealing in very dry, high-purity nitrogen and severely quenched. The Doppler broadening positron annihilation readings gave essentially the same $S$–$T$ curve as when the specimens were annealed in very dry, impure nitrogen. This indicates that the effect was not superficial and that it extended to a considerable depth.

Federighi (1965) studied the annealing of defects in a series of severely quenched aluminium-based alloys that were pre-annealed in air. He measured the resistance during isochronal annealing. In general, his annealing curves for most of the dilute alloys showed that the decrease in resistivity with increasing temperature was similar to that observed for pure aluminium. The resistivity of the quenched, dilute, solid solution, aluminium alloys started to decrease at about 200 K and was essentially restored to the value of the well annealed alloy at 350 K. This curve essentially parallels the one observed for quenched pure aluminium except that there is a small shift at higher temperatures. In contrast, small additions of magnesium in solid solution caused a significant upward displacement of about 100 K. At this temperature, the resistivity began to decrease. The resistivity as a function of temperature decreased to the value of the well annealed alloy over a wider temperature range than that observed for quenched pure aluminium and dilute aluminium–zinc and aluminium–copper alloys. Panseri *et al* (1958) found that the magnesium atoms in a quenched dilute aluminium–magnesium alloy tended to trap vacancies. This increased the post-quenched annealing temperature that is necessary to remove lattice defects. Försvoll and Foss (1967) found that there was a strong tendency for magnesium to be selectively oxidised from an aluminium–magnesium alloy, an effect not observed in aluminium–zinc alloys.

Guyot *et al* (1970), by using transmission electron microscopy, found significant changes in defect structures as the magnesium content in quenched aluminium alloys was increased. They also determined that the increasing magnesium content increased the size and stability of loops and helical dislocations.

It is thus clear that the presence of oxygen in pre-annealing atmospheres radically changes the annealing behaviour of aluminium–magnesium through external/internal oxidation. The purpose of our research was to study the nature of this oxidation process with the help of electron spectroscopy for chemical analysis (ESCA).

## 2. Experimental procedure

The specimen materials, which were provided for this research by Dr G Dlubek, consisted of two alloys of high-purity aluminium (5N) plus 500 and 1000 PPM magnesium. Before these specimens were quenched, they were heated in an atmosphere of air that had been thoroughly dried to minimise any water vapour and to remove any hydrocarbons that might react with the surfaces of the specimens. Details of the drying train are to be found in Alam *et al* (1982). The apparatus used for pre-annealing the specimens is similar to that devised by Lengeler (1976). The specimens were quenched from 850 K into hydrochloric acid chilled to 203 K with liquid nitrogen.

After the specimens were quenched, the ESCA technique was used to examine them. A Physical Electronics Model 548 was used to analyse the chemical composition of the surface oxide on the alloy, and Mg $K_\alpha$ x-rays (1253.6 eV) were employed to eject electrons from the elements present in the oxide. The binding energies of the electrons from the elements of interest and their compounds are given in table 1. The formation of compounds caused a shift to higher binding energies. The escape depth of the electrons in the

**Table 1.**

| Compound | Electron shell | Binding energy (eV) | Reference |
|---|---|---|---|
| $Al^0$ | $Al^0 2p$ | 72.65 | [a] |
| $Al_2^{3+}O_3$ | $Al^{3+} 2p$ | 74.7 | [a] |
| $Mg^{2+}O$ | $Mg^{2+} 2s$ | 89.1 | [b] |
| $Mg^{2+}Al_2^{3+}O_4$ | $Mg^{2+} 2s$ | 87.5 | [b] |
| $Al_2^{3+}O_3$ | $O^{2-} 1s$ | 531.6 | [a] |
| $Al^{3+}(OH)_3$ | $O^{2-} 1s$ | 533.3 | [a] |

[a] Wagner *et al* (1978); [b] Leonov *et al* (1978).

**Table 2.**

| Element | $S_n$ | Reference |
|---|---|---|
| O 1s | 0.63 | [a] |
| Mg 2s | 0.07 | This laboratory |
| Al 2p | 0.11 | [a] |

[a] Wagner *et al* (1978).

aluminium was about 0.9 nm for the O 1s electrons and about 0.25–0.30 nm for the Mg 2s and Al 2p electrons (Powell 1974). The energy of the electrons was analysed with a resolution of about 1 eV.

To analyse in depth, it was necessary to sputter the surfaces with an argon ion beam of 30 mA under an accelerating potential of 1 kV. The sputtered spots were about 1.5 cm in diameter. It is estimated that the sputtering rate for the specimens under these conditions was about 3.0 nm $min^{-1}$.

The analysis of the oxide relies on the relationship (Wagner *et al* 1978)

$$\frac{n_1}{n_2}=\frac{I_1/S_1}{I_2/S_2} \tag{1}$$

in which $n_n$ is the number of atoms of the $n$th element per $cm^3$ in a sample, $I_n$ the number of photons per second emitted from the $n$th element and $S_n$ the atomic sensitivity factor for the $n$th element. The value of $I_n$ for each element was obtained by integrating the area under the peak of each curve. The concentration, $C_n$, of each element can be obtained using the equation

$$C_n=\frac{n_n}{\sum_{n=1}^{n} n_n}=\frac{I_n/S_n}{\sum_{n=1}^{n} I_n/S_n}. \tag{2}$$

The values for $S_n$ are given in table 2. The value for the atomic sensitivity factor for Mg 2s was determined by using a specimen of pure MgO that had been sputtered. Measurements of the concentrations of aluminium and oxygen in aluminium oxide on pure aluminium gave a fairly consistent 40 at.% aluminium and 60 at.% oxygen concentration after removal of the oxide of 90 nm.

## 3. Experimental results

The results were obtained by using ESCA to analyse the oxides on pure aluminium plus two

alloys: Al + 500 PPM and Al + 1000 PPM magnesium. The data for pure aluminium shown in figure 1 are included to provide a basis for comparing them with the data obtained from the two alloys. The atomic fraction of oxygen (in pure aluminium) is quite high at the surface and for a distance of about 60 nm into the oxide because of the presence of chemisorbed oxygen and perhaps $Al(OH)_3$. Because the O1s peak was quite broad with no structure, there was no indication of any compound other than $Al_2O_3$. Initially, the $Al^{3+}$ 2p peak was observed at 74.7 eV. With sputtering for long periods (>60 min corresponding to a depth >180 nm), the elemental $Al^0$ 2p peak developed at 72.65 eV. This new peak, which overlapped part of the original $Al^{3+}$ 2p peak, was subtracted from the total peak area to obtain the $Al^{3+}$ 2p peak area.

Figure 2 gives the data for the alloy containing 500 PPM magnesium. Again, there is a high oxygen content on and near the surface, and this content declines to about 0.40. The aluminium content increased with depth to about the same level, while the magnesium content increased to about 0.20. The $Al^0$ 2p peak was never well developed and hence no subtraction was made from the total peak. This accounts for the higher values for aluminium and magnesium in figure 2.

An examination of the position of the Mg 2s peak indicates that it is primarily located at the electron energy corresponding to spinel, $MgAl_2O_4$ (see table 1). This compound has only 57% oxygen compared with 60% in $Al_2O_3$. With additional sputtering, the peak tended to shift a small amount to a higher energy. A small shoulder, which developed on the high-energy side, corresponded to MgO, which has a lower oxygen concentration. In as much as the magnesium content of the alloy is so low, there was no reason to expect that any elemental magnesium would be observed in the base metal.

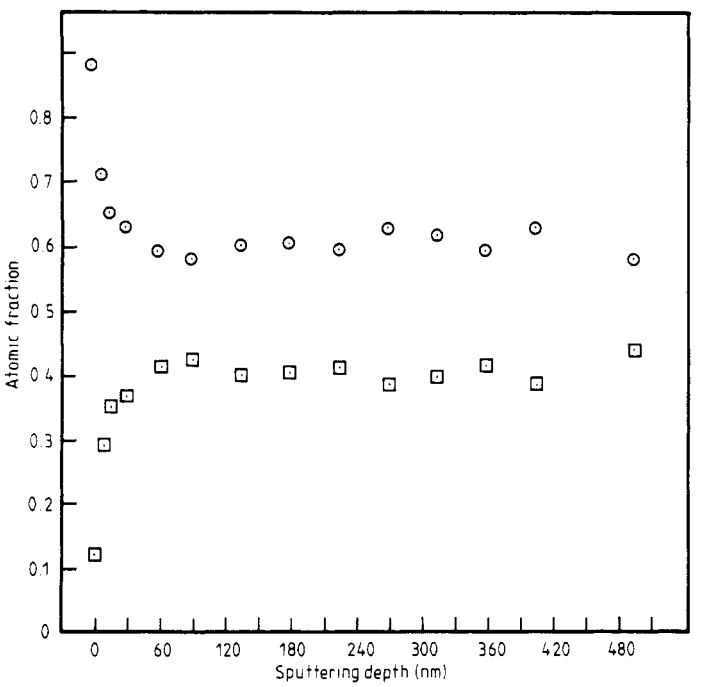


**Figure 1.** The composition of the oxide formed on pure aluminium as a function of sputtering depth: atomic fraction of oxygen (⊙) and atomic fraction of aluminium (⊡) in the surface oxide.

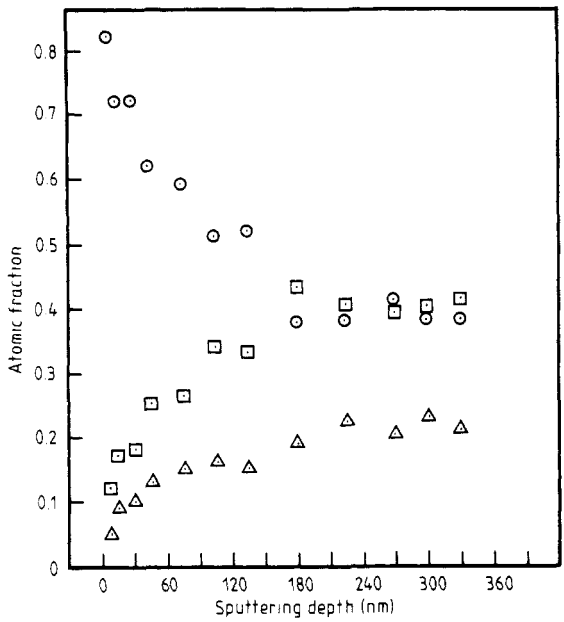


**Figure 2.** The composition of a quenched aluminium–500 PPM magnesium alloy annealed in very dry air as a function of sputtering depth: atomic fraction of oxygen (⊙), atomic fraction of magnesium (△) and atomic fraction of aluminium (⊡) in the surface oxide.

In figure 3 the data for the composition of the oxide as a function of sputtering time are given for the alloy containing 1000 PPM Mg. The decline in the oxygen content of the oxide

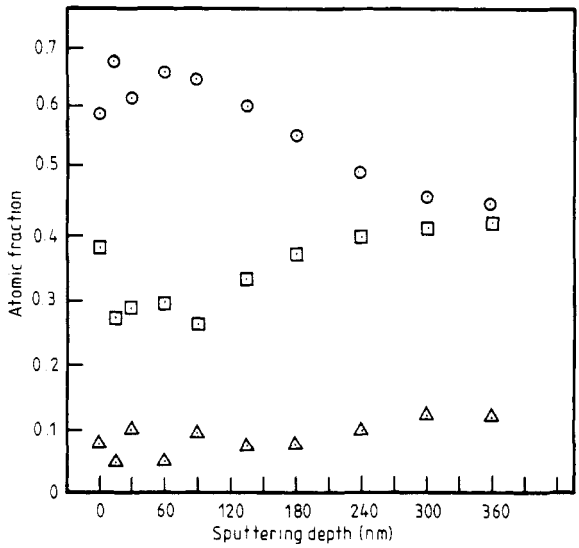


**Figure 3.** The composition of the oxide on a quenched aluminium–1000 PPM magnesium alloy annealed in very dry air as a function of sputtering depth: atomic fraction of oxygen (⊙), atomic fraction of magnesium (△) and atomic fraction of aluminium in (⊡) in the surface oxide.


**Figure 4.** The $Al^0$ 2p and $Al^{3+}$ 2p electron binding energy peaks for the aluminium–1000 PPM magnesium alloy.

was not so great as in the case of the alloy containing 500 PPM Mg, nor was the increase in aluminium content as great. The magnesium content of the oxide was not so great as in the other alloy. In this alloy, the peak for the $Al^0$ 2p peak was better developed and hence it was possible to subtract an area that represented the electrons for elemental aluminium.

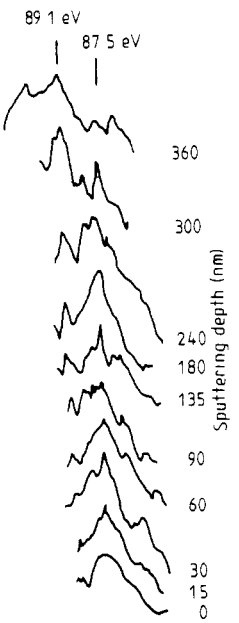


**Figure 5.** The electron binding energy spectra for MgO and $MgAl_2O_4$ as a function of sputtering depth.

Figure 4 gives an example of the $Al^0$ 2p and $Al^{3+}$ 2p electron binding energy peaks for this alloy.

In the case of magnesium, the base metal contained too small a concentration to be detectable. In the oxide, the magnesium could have been present as MgO or as spinel, $MgAl_2O_4$. For the alloy containing 500 PPM Mg, the peak was centred very nearly at 87.5 eV, which is the position predicted for spinel. There are a few instances in which there may be shoulders on the high-energy side of the peak to give a hint of the presence of MgO. Grauer and Schomaker (1976) calculated the stability regions for the system Al–Mg–$O_2$ at 800 K that are at a temperature somewhat lower than the temperature utilised for the present experiment. The spinel was the oxide in thermodynamic equilibrium with the aluminium–magnesium alloys containing $1\% \geqslant Mg \geqslant 0.0001\%$; hence the absence of MgO in this alloy was not surprising.

In the case of the alloy containing 1000 PPM magnesium the peak for the $Mg^{2+}$ in the spinel was dominant until sputtering had taken place for 100 min (a depth of about 300 nm). The $Mg^{2+}$ for MgO became apparent after sputtering for 30 min (~90 nm). These curves are shown in figure 5. The presence of MgO in the oxide does not contradict the results published by Grauer and Schomaker (1976) because they considered only equilibrium conditions.

## 4. Discussion

### *4.1. Oxide formation*

The experimentally observed presence of a large concentration of $MgAl_2O_4$ in the oxide layer of both alloys plus the large concentration of MgO in the alloy richer in magnesium can readily be explained in terms of data reported previously.

In as much as the alloys used in the present experiment were very dilute by normal standards, one should initially consider the oxidation of pure aluminium. Beck *et al* (1967) studied the oxidation of pure aluminium at high temperatures. They concluded that an amorphous $\gamma$-$Al_2O_3$ is formed in which there is a counter current flow of metal ions from the metal–oxide interface outward to the oxide–gas surface while oxide ions diffuse through the amorphous oxide to the oxide–metal interface. The growth rate obeys a parabolic relationship over the temperature range 450–575 °C.

The addition of magnesium to aluminium alters the oxidation mechanism in two ways. Försvoll and Foss (1967) showed that the magnesium atoms in aluminium are removed by diffusion when the alloy is annealed at elevated temperature. This results in a dependence of the oxidation rate of the alloy upon this diffusion. Also, Ritchie *et al* (1977) presented free energy data showing that magnesium is a sufficiently strong reducing agent to react with $Al_2O_3$ to produce MgO or preferably $MgAl_2O_4$ depending upon the composition of the alloy. Scamans and Butler (1975) observed that the nucleation and formation of $MgAl_2O_4$ crystals is much more rapid than the formation of $\gamma$-$Al_2O_3$ in pure aluminium; hence the addition of magnesium must stimulate the inward diffusion of oxygen to the metal–oxide interface.

The observed high concentrations of MgO and $MgAl_2O_4$ in the oxide, if one considers the small concentration of magnesium in the base metal, indicate that the magnesium is strongly depleted from the metal. The oxidation mechanism of the counter current flow of metal ions and oxide ions supports the data observed. Metal ions leaving the metal–oxide interface will surely leave a large concentration of vacancies behind to form defects.

### *4.2. Depletion of magnesium from the metal*

The presence of substantial concentrations of magnesium in the oxide layer as MgO and $MgAl_2O_4$ in aluminium alloys containing only 500 and 1000 PPM magnesium indicates a strong tendency for the element to diffuse to the metal–oxide interface. Because Ritchie *et al* (1977) showed that the free energy changes in the formation of these compounds exceed those for $Al_2O_3$, any magnesium crossing the metal–oxide interface would be promptly oxidised. The mechanism of Beck *et al* (1967), in which oxygen diffuses inwardly to the oxide–metal interface, would provide an abundance of oxygen to react with any magnesium atoms.

The diffusion of $^{28}Mg$ in aluminium was studied by Rothman *et al* (1974). They found the activation energy, $Q$, to be 31.15 kcal $mol^{-1}$ and the frequency factor, $D_0$, to be 1.24 $cm^2\ s^{-1}$. By using an annealing temperature of 850 K, they found that $D = 1.212 \times 10^{-8}\ cm^2\ s^{-1}$. For the depletion of the magnesium by diffusion from the aluminium, the following equation can be used as an approximate solution:

$$C(x, t) = C_0\ \mathrm{erf}(x/2\sqrt{Dt}). \tag{3}$$

Here $C(x, t)$ is the concentration as a function of distance from surface and the time for annealing (in this case 1800 s). The term $C_0$ represents the mean initial concentration and $x$ is the distance from the metal–oxide interface to the interior of the metal. Figure 6 gives the profile of the magnesium that was derived from $\mathrm{erf}(x/2\sqrt{Dt})$ as a function of $x$. Because the oxide layer is very thin, it is neglected in this plot.

To determine the amount of magnesium that diffused into the oxide—this amount is represented by the shaded area in figure 6—the following equation is used:

$$C_0 \int_0^x \left(1 - \mathrm{erf}\left(\frac{x}{2\sqrt{Dt}}\right)\right) dx = C_0 \int_0^x \mathrm{erfc}\left(\frac{x}{2\sqrt{Dt}}\right) dx = \frac{C_0\sqrt{Dt}}{\Gamma(\frac{3}{2})} = 1.1 C_0 \sqrt{Dt}. \tag{4}$$

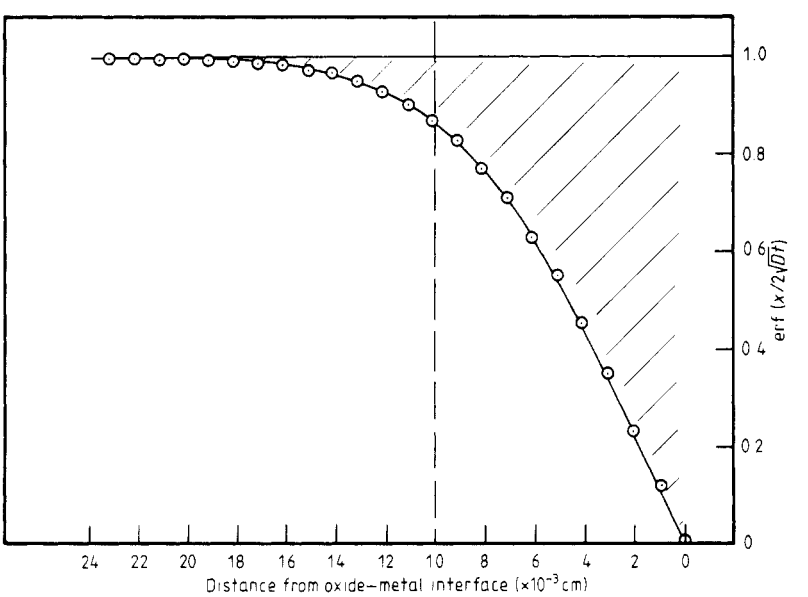


**Figure 6.** The profile of $\mathrm{erf}(x/2\sqrt{Dt})$ as a function of $x$ for magnesium in aluminium heated in dry air at 850 K for 30 min.

By evaluating this equation with $C_0 = 1000$ PPM, it can be shown that $3.09 \times 10^{17}$ magnesium atoms $cm^{-2}$ leave the alloy to form MgO and $MgAl_2O_4$ in the oxide layer during the period of annealing (850 K for 30 min).

The magnesium atoms leaving the metal to enter the oxide leave vacancies which tend to enter the metal. If one assumes that these vacancies are in the outermost 0.2 cm layer, the vacancy concentration would be about $2.565 \times 10^{-5}$ which is about the value of the vacancy concentration in the defects observed by Guyot *et al* (1970), who used electron microscopy to examine an alloy of aluminium–magnesium quenched from 823 to 263 K.

As noted earlier, the removal of about 0.01 cm from the surface by abrasion has no significant effect on the $S$–$T$ curve as observed by positron annihilation spectrometry. Examination of figure 6 shows that, after removal of 0.01 cm, a volume depleted in magnesium would still remain. A second annealing in very pure nitrogen permits magnesium atoms to diffuse outward and vacancies to diffuse inward. With this condition, clustering is likely because the concentration is somewhat greater than the equilibrium value. Quenching retains the clusters, which trap positrons and increase the parameter $S$. Because the amount removed is only approximate, greater numbers of vacancies may exist.

### *4.3. Summary of defects in aluminium–magnesium alloys*

As noted earlier, Alam *et al* (1982) used positron annihilation spectrometry to study the effect of oxygen on the annealing behaviour of quenched aluminium–magnesium alloys. The $S$–$T$ curves for such alloys, which are annealed in very dry, very pure nitrogen before they are quenched, are very similar to curves for aluminium–zinc and aluminium–copper alloys, whereas the presence of oxygen in the annealing atmosphere brings out very significant changes in the $S$ parameter as a function of temperature. This is indicative of large increases in the defect concentration.

This has been discussed previously in connection with the formation of MgO and $MgAl_2O_4$ in the $\gamma$-$Al_2O_3$ surface of an alloy. The migration of metal ions from the metal–oxide interface to the oxide surface will leave large numbers of vacancies behind. Dobson *et al* (1968) observed the growth of vacancy loops during annealing in quenched aluminium–magnesium alloys. The growth is in contrast to loop shrinkage normally observed in quenched aluminium and its other alloys. These authors concluded that surface oxidation of the magnesium generates vacancies at the metal–oxide interface. Kritzinger and Ronander (1978) observed similar growth of loops even when annealing occurred in a vacuum of $10^{-6}$ Torr. They noted the growth of MgO as a consequence of annealing in oxygen at a pressure of approximately one atmosphere. Guyot *et al* (1970) observed large numbers of prismatic vacancy loops in alloys of aluminium plus magnesium quenched from 550 °C. Large increases in magnesium content in the alloy reduced the numbers, diameter and inferred vacancy concentration. The resistivity after isochronal annealing showed a significant retardation in recovery with increasing magnesium content. Annealing after quenching indicated a trapping of vacancies by impurity atoms in as much as the number, diameter and inferred vacancy concentration were greater for annealing at 100 °C as compared with annealing at 20 °C. Panseri *et al* (1958), in performing resistivity measurements on quenched aluminium–magnesium alloys, showed that increased magnesium content increases the change in resistivity because of an increased number of retained vacancies at quenching. Because they made no attempt to protect the specimens' preferential oxidation of the magnesium, large numbers of vacancies would have been injected into the base metal as the result of surface oxidation.

## 5. Conclusions

The oxidation of alloys of aluminium containing small concentrations of magnesium shows a very strong preference for the depletion of magnesium from the alloy. The magnesium appears in the oxide layer as spinel, $MgAl_2O_4$, near the oxide–oxygen interface. With increasing depth in the oxide, MgO begins to appear and, in the case of the alloy containing 1000 PPM of magnesium, MgO becomes the predominant magnesium-containing compound.

An analytical treatment of the magnesium depletion from the alloy discloses a value essentially equal to the magnesium appearing in the oxide layer. This depletion of magnesium atoms from the alloy injects vacancies into the alloy that produce defect structures. These defect structures have been observed by other investigators directly by electron microscopy and indirectly by resistivity measurements and positron annihilation.

## Acknowledgment

The kind assistance of H Rice in producing the ESCA spectra is acknowledged.

## Appendix

In Doppler broadening positron annihilation spectroscopy, one obtains from metallic specimens a broad peak of annihilation $\gamma$-ray intensity as a function of the energy of the annihilation $\gamma$ rays by using appropriate counting techniques including a multichannel analyser. This peak is centred at 511 keV. The deviation of the $\gamma$-ray energy from the ideal 511 keV is a consequence of the conservation of energy of the annihilation electron–positron annihilation interactions. To quantify these results, the $S$ parameter is results from core-electron–positron annihilation interactions, whereas the central part of the peak can be fitted to a parabolic-shaped curve which results from the valence-electron–positron annihilation interactions. To quantify these results, the parameter $S$ is used. This is defined as the ratio of the number of counts in the central 12 channels to the total number of counts (MacKenzie *et al* 1970). The defects (point defects and defect clusters) act as traps from the positrons and thus increase the probability of valence-electron–positron annihilation events while reducing the core-electron–positron annihilation rate, thereby increasing the $S$ parameter.

## References

Alam A, Leighly H P Jr and West R N 1982 *J. Phys. F: Met. Phys.* **12** 399
Alam A and West R N 1982 *J. Phys. F: Met. Phys.* **12** 289
Beck A F, Heine M A, Caule E J and Pryor M J 1967 *Corrosion Sci.* **7** 1
Dobson P S, Kritzinger S and Smallman R E 1968 *Phil. Mag.* **17** 769
Federighi T 1965 *Lattice Defects in Quenched Metals* ed. R M J Cotterill *et al* (New York: Academic) p 217
Försvoll K and Foss D 1967 *Phil. Mag.* **15** 219
Grauer R and Schomaker P 1976 *Werkstoffe und Korrosion* **27** 769
Guyot P, Fremiot M and Wintenberger M 1970 *Proc. 7th Int. Congr. on Electron Microscopy, Grenoble* p 253
Kritzinger S and Ronander R 1978 *Proc. 9th Int. Congr. on Electron Microscopy, Toronto* ed. J M Sturgis vol. 1 p 448

Lengeler B 1976 *Phil. Mag.* **24** 259
Leonov A I, Kostikov Yu P, Trusova E M, Ivanov I K and Andreeva N S 1978 *Izv. Akad. Nauk SSSR, Neorganisheskie Materialy* **14** 498
MacKenzie I K, Eady J A and Gingerich R R 1970 *Phys. Lett.* **33A** 279
Panseri C, Gatto F and Federighi T 1958 *Acta Metall.* **6** 198
Powell C J 1974 *Surf. Sci.* **44** 29
Ritchie I M, Sanders J V and Weickhardt P L 1977 *Oxidation of Metals* vol. 3 (New York: Pergamon) p 91
Rothman S J, Peterson N L, Nowicki L J and Robinson L C 1974 *Phys. Status Solidi* b **63** K29
Seamans G M and Butler E P 1975 *Metall. Trans.* A **6** 2055
Wagner C D, Riggs W M, Davis L E, Moulder J F and Muilenberg G E 1978 *Handbook of X-Ray Photoelectron Spectroscopy* (Eden Prairie, Minnesota: Perkin–Elmer)
West R N 1979 *Positron Studies of Lattice Defects in Metals, Positrons in Solids* ed. P Hautojärvi (Berlin: Springer) p 89